Article
https://doi.org/10.31489/2024PH4/156-167
UDC 628.9.037

Received: 06.06.2024
Accepted: 09.08.2024

E.F. Polisadova, N.D. Tran

National Research Tomsk Polytechnic University, Tomsk, Russia
*(*Corresponding author's e -mail: elp@tpu.ru)*

Electron Beam-assisted Synthesists, Structure and Luminescent Properties Porous Ceramics of $MgAl_2O_4$ and $MgAlGaO_4$ Doped with Europium

Porous ceramics of $MgAl_2O_4$ (MAS) and $MgAlGaO_4$ (MAGS) doped with europium were synthesized by radiation method. Radiation synthesis was performed with high efficiency within less than 1 s using radiation energy and mixture materials with no additives or any other materials used to promote synthesis. The synthesis method using a high-energy electron beam makes it possible to obtain refractory materials with high productivity, flexibly control the technological conditions of the process, and, accordingly, synthesize materials with desired properties. The structural properties of synthesized porous ceramics were investigated by X-ray diffraction (XRD-7000S diffractometer, Shimadzu), SEM. Results have shown that, the synthesized MAS have cubic structure and are in crystalline spinel $MgAl_2O_4$, while the synthesized double spinel MAGS contains two main phase components, $MgAl_2O_4$ and $MgGa_2O_4$. To study the luminescence properties of MAS and MAGS synthesized spinel doped with europium, photoluminescence measurements were performed. The photoluminescence spectrum of excitation of Eu^{3+} ions in spinel was monitored at λ_{em} = 615 nm ($^5D_0 \rightarrow {}^7F_2$). The PLE shows the f→f transition in the configuration of Eu^{3+} ions (at 393 nm ($^7F_0 \rightarrow {}^5L_6$), 463 nm ($^7F_0 \rightarrow {}^5D_2$)). The excitation band at 330 nm and 260 nm is characteristic of the charge transition between Eu^{3+} and O^{2-} ions. The photoluminescence spectrum of the samples under excitation at 260 nm was studied. In the PL spectrum of spinel samples, the emission of Eu^{3+} ions are clearly visible. In the structure of the band with a maximum of 615, a peak is visible at 590 nm, characterized by the $^5D_0 \rightarrow {}^7F_1$ transition. In the PL spectrum of samples, a weak spectral band appears with a maximum at 535 nm, characteristic of the emission of Eu^{3+} ions with the $^5D_1$-$^7F_1$ transition. It is shown that the efficiency of radiation synthesis depends on the granulometric composition of the initial oxide powders.

Keywords: ceramic spinels, double spinel, Eu-doped, radiation synthesis, luminescence, MgAl2O4, MgAlGaO4.

Introduction

Materials with spinel structure are technologically significant materials in science and technology. Aluminum-magnesium spinel $MgAl_2O_4$ has high hardness, chemical stability, low electrical conductivity, resistance to temperature effects, spinel crystals are transparent in the visible and infrared wavelength ranges [1]. Due to the combination of optical, mechanical and thermal properties, aluminum-magnesium spinel is used in aviation and space technology, optical elements of optical and optoelectronic devices operating in extreme conditions, gas sensors, and active laser media are produced from it. Design of materials in the form of double spinels opens up great prospects. In [2, 3], theoretical methods showed that the double spinel structure is thermodynamically favorable for the mixed system $MgAl_2O_4$ + $MgGa_2O_4$, mixing of cations on different sublattices will occur at a relatively low temperature. Synthesis of such materials opens up new possibilities for designing materials with spinel structure and individual functionality.

The authors of [4] showed that double aluminum-gallium-magnesium spinel $MgAlGaO_4$ spinel has semiconductor properties and is a promising material for manufacturing short-wave LED and laser devices, photovoltaic solar cells. However, the technologies for synthesizing such materials are not developed. Synthesis of materials based on normal $MgAl_2O_4$ and inverse $MgGa_2O_4$ spinel is carried out by thermal [5] and sol-gel [6] methods. The methods are complex and labor-intensive. In [5, 6], it was shown that partial conversion occurs in inverse spinel $MgGa_2O_4$: Mg^{2+} and Ga^{3+} can occupy tetrahedral and octahedral positions, which facilitate the penetration of the dopant and changes the luminescent properties. In [5], it was shown that $MgGa_2O_4$ doped with Eu^{3+} ions has excellent luminescent properties in the "red" and "orange" regions of the spectrum, $MgGa_2O_4$: Mn^{2+} phosphors were successfully used as green emitters in night vision and data storage devices, and in [7], inverse spinel was proposed to be used as a self-activating phosphor. Europium-

activated $MgAl_2O_4$ spinel is a promising heat-resistant phosphor [8]. The luminescent properties of double spinel $MgAlGaO_4$ have not yet been studied.

This paper considers the possibility of using a radiation method using a high-energy electron beam to synthesize ceramics based on $MgAl_2O_4$ and double spinel $MgAlGaO_4$. The synthesis method has been well tested on refractory oxide materials [9, 10]. The method is characterized by high synthesis speed and high efficiency.

Experimental

The radiation method of synthesis is based on the ability of high-energy particles to excite and destroy molecules of a substance, leading to the formation of new materials. For example, an electron penetrates a substance, causing ionization in it: the particle forms about 10 thousand particles of lower energy, these particles begin to break old chemical bonds and form new ones. Therefore, the use of the energy of an electron beam generated by an accelerator for the synthesis of ceramics from refractory inorganic materials is very promising and this method is used to synthesize spinel samples in our study. The synthesis of ceramics was carried out by direct action of an electron beam on the initial mixture of a given composition on the ELV6 electron accelerator at the facility UNU Stand ELV-6 at the Budker Institute of Nuclear Physics SB RAS [11]. High-energy electron beams with an electron energy of 1.4 MeV were used for synthesis. The resulting beam was extracted through a differential pumping system, had a Gaussian profile on the target surface with a spot area of 1 cm². The synthesis occurred when the threshold power density of the energy flow was exceeded, which was 30 kW/cm². For the synthesis process, a mixture of high-purity oxides MgO, Al_2O_3 and Ga_2O_3 in a stoichiometric ratio was prepared. Eu_2O_3 oxide was added to the mixture in an amount of 0.5 wt.%. The oxide mixture was stirred in a mixer for 2 hours, after which it was placed in a massive copper crucible measuring 100 × 50 × 10 mm. The crucible depth for the synthesis of a specific ceramic was selected based on the condition of complete absorption of the electron beam of a given energy by the mixture. The crucible was located under the accelerator outlet on a strong metal table. Synthesis proceeds in two different modes: "scanning" and "no scanning". In the "no scanning" mode, the crucible displaces relative to the beam at a speed of 1 cm/s along the entire length of 100 mm. In the "scanning" mode, the beam scans in the transverse direction of the scanning beam. The beam cross section is 1 cm^2 in the plane of the crucible surface. The electron beam was scanned at a frequency of 50 Hz in the transverse direction of the crucible, while the crucible moved relative to the scanning beam at a speed of 1 cm/s.

The structure of the obtained samples was studied using an XRD-7000 X-ray diffractometer (Shimadzu, Japan). The morphology of the samples was studied using a Hitachi TM3030 scanning electron microscope CEM with a Bruker XFlash MIN SVE energy dispersive analysis system at an accelerating voltage of 15 kV. The dispersion of all starting materials was measured by laser diffraction on a Shimadzu SALD-7101 laser particle size analyzer.

Cathodoluminescence (CL) was measured using a pulsed electron beam from the GIN-600 accelerator as an excitation source. The electron pulse duration at half-width $t_{1/2}$ was 15 ns, the average energy of accelerated electrons E was 250 keV, and the electron beam power density was j = 8 — 300 mJ/cm^2. Cathodoluminescence oscillograms were recorded at a certain wavelength in the range of 250–1100 nm by an optical spectrometer consisting of an MDR-3 monochromator, an FEU-106 photomultiplier, and a four-channel 350 MHz LeCroy WR 6030A oscilloscope. The oscillograms were then converted into luminescence kinetic curves in order to determine the kinetic parameters of luminescence decay. The integral CL spectra were measured using an AvaSpec-2048 fiber-optic spectrometer (340–1100 nm) in a "time window" 1 ms. All measured data were corrected taking into account the spectral sensitivity of the optical path.

The photoluminescence (PL) and excitation spectra were measured using an Agilent Cary Eclipse fluorescence spectrophotometer. The spectrophotometer uses a high-performance R928 dual photomultiplier with a scanning speed of 24,000 nm/min, a pulsed xenon flash lamp with a frequency of 80 Hz is used, the spectral range of the spectrometer is from 190 to 1100 nm.

Results and Discussion

In this work, several samples of spinels, normal and double, were synthesized and studied using initial components with different dispersion and under different process conditions. Table 1 shows the compositions and designations of the samples and initial components.

The study of the structure of the synthesized radiation ceramics showed that the position of the diffraction peaks of the MgAl2O4 samples and their intensity completely correspond to the X-ray diffraction pattern of the reference sample of spinel $MgAl_2O_4$ from the PDF2 database (card 00-021-1152). The synthesized samples have a cubic structure belonging to the F3dm group with a lattice constant corresponding to the sample in the PDF2 database. In addition to the diffraction peaks corresponding to the reference sample of spinel, there is also a diffraction peak at $2\theta = 43.04$, attributed to the flat reflection (200) of the MgO phase. Clear diffraction peaks indicate good crystallinity of the synthesized $MgAl_2O_4$. Weak peaks of the MgO phase and the absence of peaks associated with Al_2O_3 indicate a sufficiently high purity of the obtained $MgAl_2O_4$. The average crystallite size of the synthesized samples is in the range of 500–600 nm.

Table 1

Ceramics synthesized by radiation method

Type spinel	Sample	Type powder			Composition	Power kW/cm^2	Sample weight, g.	Output %
		MgO	Al_2O_3	Ga_2O_3				
$MgAlGaO_4$	MAGS1	M2	K7	K8	MgO 35.9 %, Al_2O_3 22.8 %, Ga_2O_3 41.3 %, Eu_2O_3 0.5 %	7	-	-
$MgAlGaO_4$	MAGS2	M2	K7	K8		30	43.4	97.1
$MgAl_2O_4$	MAS1	M2	F800/10	-	MgO 28.4 %, Al_2O_3 70.6 %, Eu_2O_3 0.5 %	7	-	-
$MgAl_2O_4$	MAS2	M2	F800/10	-		30	27.9	56.6
$MgAl_2O_4$	MAS3	K11	K7	-		7	-	-
$MgAl_2O_4$	MAS4	K11	K7	-		30	26.1	98.1

SEM images of MgAl2O−4: Eu3+ ceramic samples with different initial oxide powder compositions (MAS2 and MAS4) are shown in Figure 1. The surfaces of the samples have complex shapes characteristic of a solidified melt. The difference in the surface morphology of the synthesized samples can be explained by changes in the structural and phase composition from sample to sample.

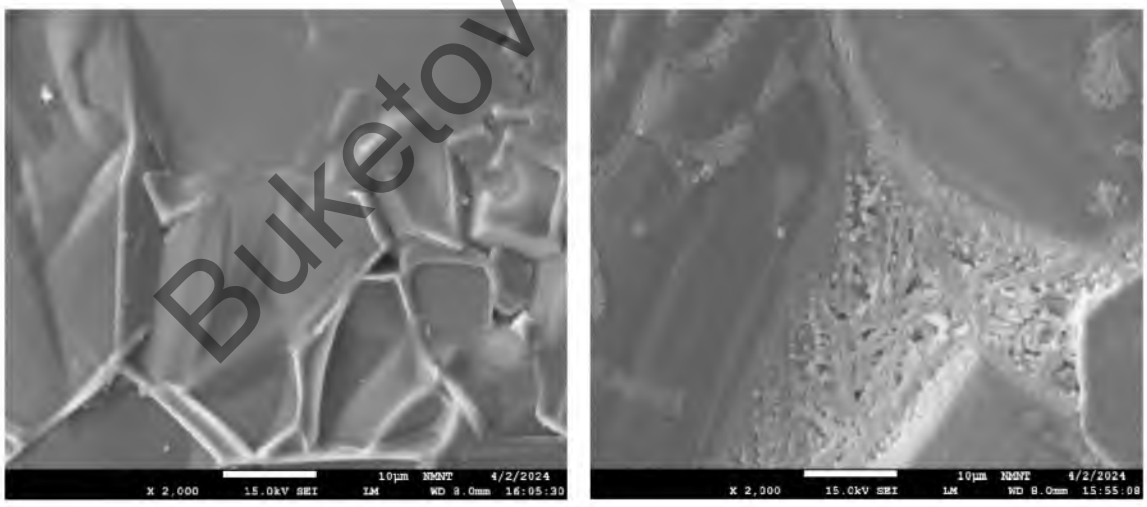

Figure 1. SEM images of the surface of MgAl2O-4: Eu3+ ceramic samples with different initial oxide powder compositions (MAS2 and MAS4)

Figure 2 shows the element distribution maps obtained with a scanning electron microscope. The microphotographs show that the surface layer contains Mg, Al, O. The introduced Eu impurities are distributed non-uniformly over the surface. During the synthesis, the Eu oxide dissociates and the Eu^{3+} and O^{2-} ions enter the spinel matrix independently of each other.

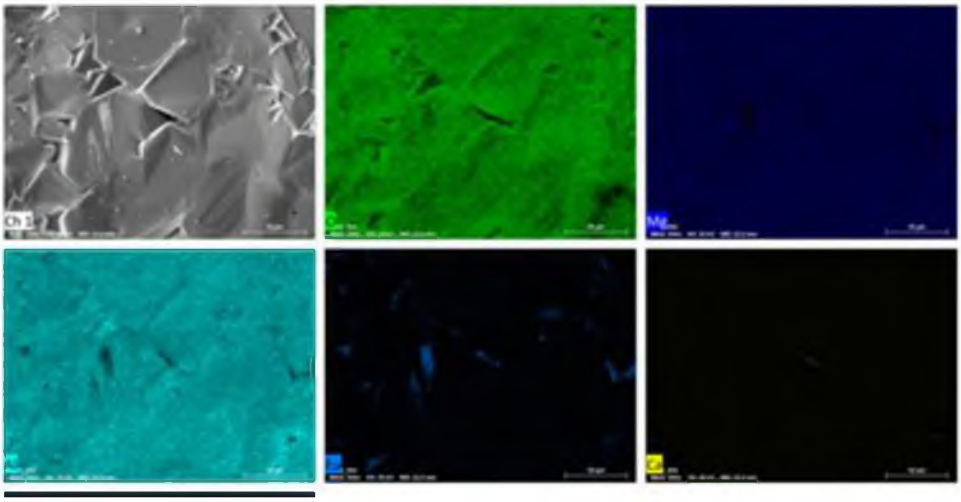

Figure 2. Result of mapping the distribution of elemental composition in the $MgAl_2O_4$: Eu^{3+} spinel sample (MAS2)

The elemental composition of the studied MgAl2O4: Eu3+ samples obtained by energy-dispersive analysis are shown in Figure 3. The energy-dispersive X-ray analysis spectra show elemental peaks, confirming the presence of Mg, Al, O, Eu and several impurity elements.

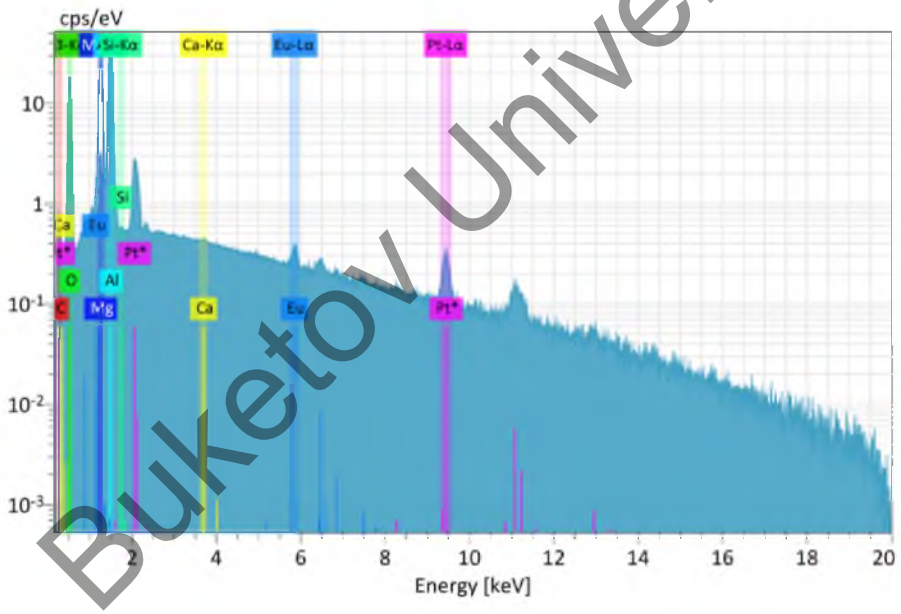

Figure 3. The elemental composition of the studied $MgAl_2O_4$: Eu^{3+} samples obtained by energy-dispersive analysis

Table 2

Mass composition of samples $MgAl_2O_4$: Eu^{3+}

Element	Mass (%)	Atom (%)
Oxygen (O)	37,27	50,39
Magnesium (Mg)	14,67	13,06
Aluminum (Al)	32,99	26,45
Silicon (Si)	0,03	0,02
Calcium (Ca)	0,02	0,01
Europium (Eu)	0,84	0,12
Platinum (Pt)	5,11	0,57

Quantitative elemental analysis of the samples allowed us to establish the composition of the ceramics, the data of which are shown in Table 2. The results show that the composition of the elements is uniformly distributed. The percentage of elements obtained in the samples is similar to the theoretical calculation.

The work investigated the efficiency of synthesis from the history of the initial oxide powder compositions with different particle sizes, as well as partial replacement of Al3+ with Ga3+. The symbols for the synthesized spinel samples are presented in Table 3. The efficiency of the synthesis process was determined as the ratio of the mass of the sample obtained after synthesis to the mass of the initial powder mixture of oxides according to the formula: Efficiency (Output) (%) = M_s/M_m 100 %, where M_s is the mass of the synthesized sample, M_m is the mass of the mixture.

Table 3

The average particle size and particle sizes for the distribution maximum

Powder	Grain sizes of starting substances, μm	Average particle diameter (μm)	Particle sizes at distribution maximum (μm)
MgO (M2)	0.05 — 60	4.697	22.795
MgO (K11)	0.01 — 30	2.327	3.564
Al2O3 (K7)	0.01 — 30	2.623	9.992
Al2O3 (F800/10)	0.5 — 20	8.103	9.992
Ga2O3 (K8)	0.1 — 50	5.037	6.232
Eu2O3 (K2)	0.01 — 20	0.523	2.008

In [9, 12], it was shown that the efficiency of YAG ceramic synthesis depends on the particle sizes of the powders. This hypothesis was tested on ceramics based on two types of spinels. The dispersion of the initial powders used for synthesis to obtain the ceramic samples was studied. The average particle size and the particle sizes at the maximum of the distribution are shown in Table 3.

Figure 4 shows photographs of the synthesized samples of MAGS2, MAS2, MAS4 in crucibles. The photographs demonstrate the appearance of the samples synthesized in the “scanning” mode under the action of electron beams with E = 1.4 MeV and a flux power density of 30 kW/cm2. The synthesized samples are porous ceramics, have the appearance of complex-shaped polycrystalline plates, the size is determined by the dimensions of the crucible. In order for the crucible material not to pass into the batch during synthesis, the thickness of the powder mixture layer was always greater than the electron path depth. Therefore, a layer of batch residues always remained between the bottom of the crucible and the lower surface of the sample. The MAS2 sample is characterized by the formation of ceramics in the volume of the mixture layer, the presence of powder residue on the ceramic surface (Fig. 4).

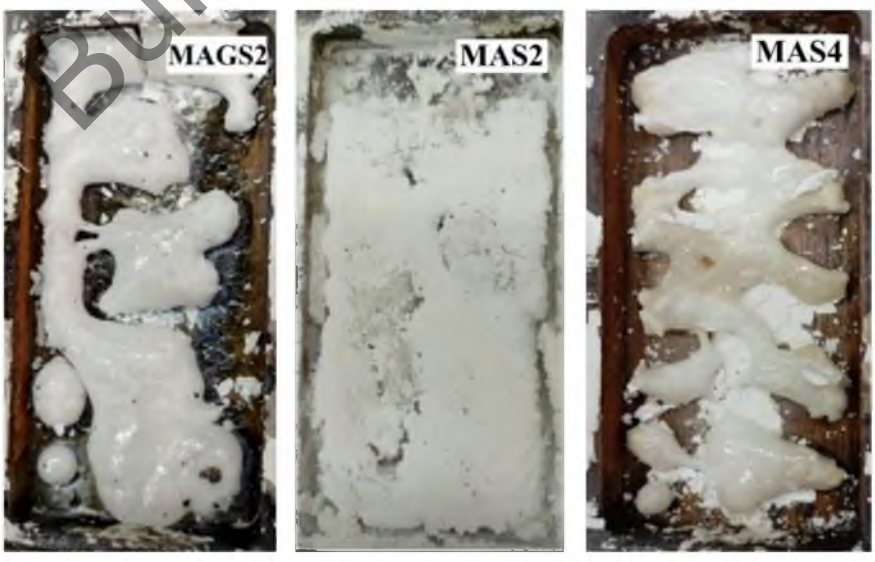

Figure 4. Photographs of synthesized spinel ceramics

A large difference in the efficiency of sample synthesis is observed depending on the granulometric composition. The synthesis results (Output) are given in Table 1. Aluminum oxide powder (K7) and magnesium oxide powder (K11) have the same average particle size and close particle size dispersion, which ensures high efficiency of radiation synthesis, sample MAS4 (98 %). Sample MAGS2 is synthesized from magnesium oxide powder (M2), aluminum oxide powder (K7) and gallium oxide powder (K8) with close average particle sizes and also has a high synthesis efficiency of up to 97 %. Aluminum oxide powder (F800/10) and magnesium oxide powder (M2) have significantly different average particle sizes (Table 3), the particle size differs by about two times, in addition, the M2 powder contains large particles (23 μm). This ratio of the particle sizes of the original powders leads to the fact that therefore the MAS2 spinel synthesized from this mixture of oxides has a rather low yield of 56 %. The reason for the dependence of the efficiency of synthesis of ceramics of complex compositions on the particle size is the difference in the dispersion of the powders of the initial compositions. When the sizes of the batch components of different chemical compositions differ significantly, local non-stoichiometry may occur, since large particles are surrounded by many small ones [12], respectively, the irradiation conditions for particles of different sizes are not identical. In addition, when filling and preparing the batch into the crucible, uneven distribution of large and small particles by volume may be observed. The dispersion composition of the activator, europium oxide, does not have a large effect on the efficiency of radiation synthesis, since it is introduced into the batch in a small amount. However, the radiation synthesis modes can affect the processes that determine the incorporation of the europium ion into the spinel lattice.

Cathodoluminescence

The cathodoluminescence characteristics of the ceramic samples were investigated. The results are presented in Figure 5. The analysis was performed for the luminescence spectra of the samples synthesized in two modes: “scanning” and “no scanning”. It was found that the luminescent properties of the sample pairs obtained in the “scanning” and “no scanning” modes are mainly qualitatively similar. The CL analysis showed that the luminescence spectra of MgAlGaO4 and MgAl2O4 spinels are similar (Fig. 5a, c) (samples MAGS1, MGAS2 and MAS3, MAS4). The spectra contain glow bands with maxima at 520, 615 and 710 nm, the ratio of band intensities can vary for the samples obtained under different conditions. In particular, samples MGAS2 and MAS4 demonstrated high synthesis efficiency (Table 1). The qualitative composition of the CL spectra in samples MAS1 and MAS2 is different (Fig. 5b); the spectrum is dominated by emission with a maximum at 690 nm and a set of peaks in the 690–800 nm region, which is associated with the luminescence of the chromium ion [13].

In samples MAGS1, MGAS2 and MAS3, MAS4, the dominant luminescence spectrum is a narrow band at 615 nm, caused by the luminescence of europium ions. In samples MAS1 and MAS2, a weak band is observed at 615 nm and an intense band in the 690–800 nm region with a maximum in the 690 nm region.

It is known that the presence of the dopant Eu3+ in the spinel lattice causes intense luminescence due to the $^5D_{0.1} \rightarrow {}^7F_J$ transitions (615 nm band) in europium ions [5, 6, 8]. Samples MAS1 and MAS2 differ from other types of synthesized ceramics. For their synthesis, F800/10 aluminum oxide was used. Al2O3 (F800/10) powders have a larger average particle size compared to magnesium oxide and a distinct difference in particle size distribution with MgO (M2). In this case, Al2O3 (K7) and MgO (K11) powders with a close average particle size and similar size distribution were used to synthesize samples MAS3 and MAS4. Apparently, a significant difference in the average particle size of the powders can affect both the formation of the spinel crystal lattice during radiation synthesis and the activation of spinel by Eu^{3+} ions. Intense luminescence in the 615 nm band associated with impurity Eu3+ ions (transition $^5D_0 \rightarrow {}^7F_2$) is recorded in the MAGS1, MAGS2, MAS3 and MAS4 samples. This band is observed in samples MAS1 and MAS2, but its intensity is weak compared to the luminescence in the 690 nm band. Thus, it can be concluded that the method of spinel synthesis using a high-energy electron beam does not affect the appearance of the spectral bands, but changes the intensity ratio of the luminescence bands of impurity and intrinsic centers. The ratio of luminescence intensities between the spectral bands with maxima at 615 nm and 710 nm differs significantly for samples synthesized at different power densities: 4:1 for MAGS1 at 7 kW/cm2, 2:1 for MAGS2 at 30 kW/cm2. For samples MAS3 and MAS4, the effect of the method of action on the luminescence intensity is insignificant, i.e. the intensity ratio I_{615} / I_{710} is ~ 2:1 (Fig. 5). A band at 520 nm can also be recorded in the CL spectra; in [14], the authors associate this luminescence with oxygen vacancies in the spinel structure.

A band at 380 nm is recorded in the CL spectra of $MgAlGaO_4$ samples, while it is absent in $MgAl_2O_4$ samples. In [15] luminescence in the CL spectra of $MgGa_2O_4$ crystals is recorded in the range of 300–

450 nm with a maximum at ~362–393 nm, depending on the annealing conditions of the crystals. The authors associate the change in the peak position in this spectral region with the redistribution of cations in the inverted spinel structure and the corresponding differences in the localization energies of self-trapped excitons. $MgGa_2O_4$ phases can appear in the composition of $MgAlGaO_4$ ceramics during synthesis, which causes the appearance of a band with maximum 380 nm in the CL spectrum. In the CL spectrum of the MAS3 and MAS4 samples, a band is observed in the region of 440–460 nm. The luminescence in the region of 460 nm is due to the luminescence of clusters formed as a result of the interaction of F^+ centers with nearby negatively charged defects in the cationic sublattice of spinel [16]. In [16], the band in the spectrum of the $MgAl_2O_4$ phosphor with a maximum at 440 nm was attributed to luminescence centers in the form of Mg^{2+} vacancies.

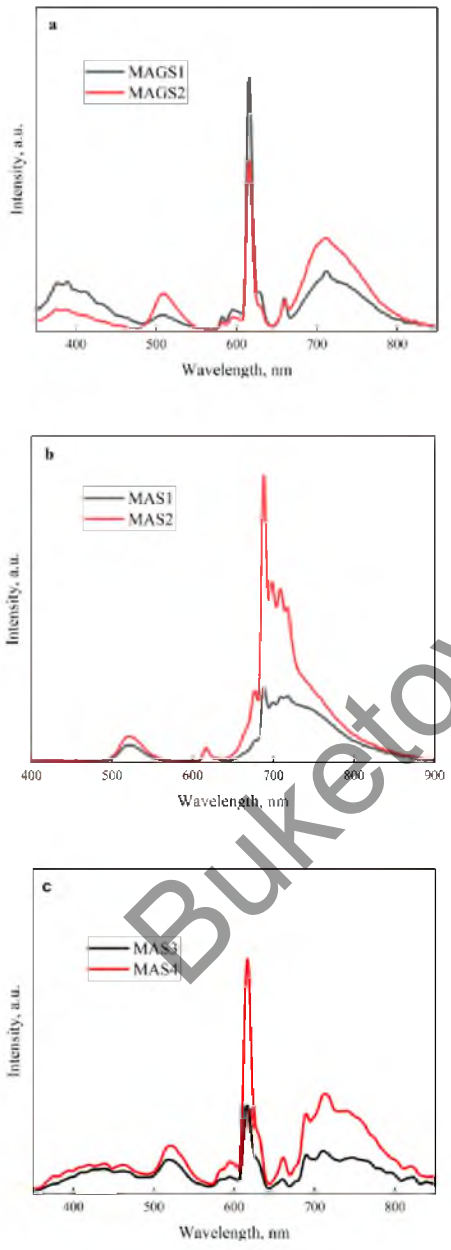

Figure 5. CL spectrum of samples: a) MAGS1 and MAGS2, b) MAS1 and MAS2 and c) MAS3 and MAS4

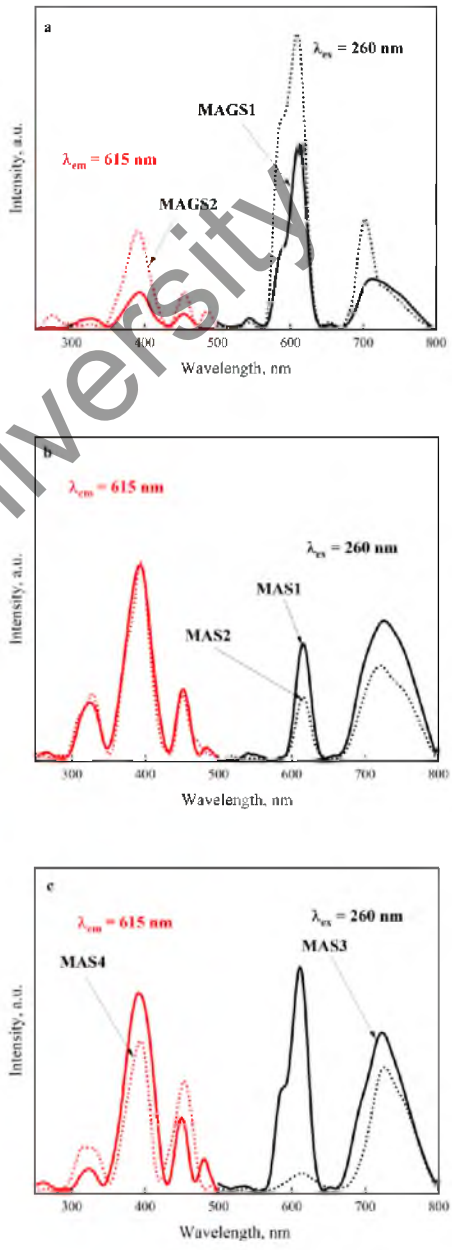

Figure 6. Excitation and PL spectrum at λ_{em} = 615 nm and λ_{ex} = 260 nm of samples: a) MAGS1 and MAGS2, b) MAS1 and MAS2 and c) MAS3 and MAS4

The kinetics of luminescence decay under pulsed electronic excitation in the region of 615, 690, and 710 nm has been studied. Luminescence can be described by the sum of two exponential components. Fig-

ure 7 presents the obtained results. In the region of 615, 690, and 710 nm, the characteristic decay times in the range up to 5 μs for each individual sample synthesized with different power densities are similar. It was found that the shape of the CL kinetic curves in the 615 and 710 nm band significantly differs for MAGS1, MAGS2, and MAS3 and MAS4 samples.

Table 4 summarizes the kinetic decay times for all the samples studied. In the spectral ranges of 615 and 710 nm, the $MgAlGaO_4$ spinel sample shows the largest decay time compared to other samples. The decay time of the $MgAlGaO_4$ spinel sample reaches its maximum in the spectral range with a maximum of 615 nm; the decay time of the fast component τ_1 and the slow component τ_2 in MAGS1 and MAGS2 samples in the 615 nm band is $\tau_1 \approx 0.1$ μs and $\tau_2 \approx 0.9$ μs.

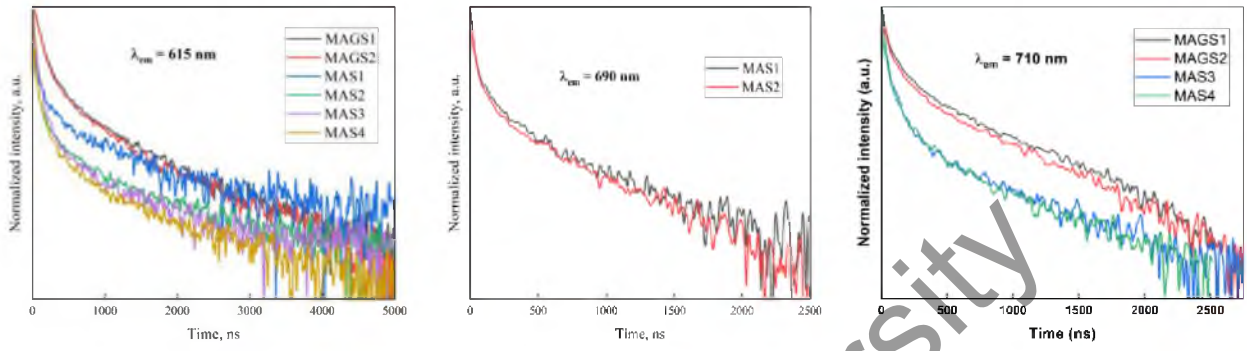

Figure 7. Kinetic characteristics of CL decay MAGS1, MAGS2, MAS1, MAS2, MAS3 and MAS4 in the region of 615, 690, 710 nm

Table 4

Luminescence decay time of MgAlGaO4 and MgAl2O4 ceramic samples in the characteristic bands

Sample	615 nm		690 nm		710 nm	
	τ1 (ns)	τ2 (ns)	τ1 (ns)	τ2 (ns)	τ1 (ns)	τ2 (ns)
MAGS1	120	902	-	-	41	453
MAGS2	118	896	-	-	38	436
MAS1	30	624	25	343	-	-
MAS2	23	421	24	352	-	-
MAS3	39	315	-	-	26	241
MAS4	24	320	-	-	25	275

Photoluminescence

Photoluminescence and excitation spectra (PL) of the synthesized spinel samples were studied. The photoluminescence excitation spectrum of Eu^{3+} ions in spinel was monitored at an emission wavelength of 615 nm (transition $^5D_0 \rightarrow {}^7F_2$). In the photoluminescence excitation spectrum, bands with a maximum at wavelengths of 393 nm ($^7F_0 \rightarrow {}^5L_6$), 463 nm ($^7F_0 \rightarrow {}^5D_2$) are recorded, corresponding to the f→f configuration transitions in the Eu^{3+} ion. Excitation bands at 330 nm and 260 nm are characteristic of the charge transition between Eu^{3+} and O^{2-} ions [17]. The PL spectrum of the samples at excitation at 260 nm was studied. Luminescence bands of Eu^{3+} ions appear in the emission spectrum of the spinel samples. In the structure of the band with a maximum at 615, a peak at 590 nm is observed, characterized by the transition $^5D_0 \rightarrow {}^7F_1$. In the PL spectra of all samples, a weak spectral band with a maximum at 535 nm appears, characteristic of the emission of europium ions with the transition $^5D_1 \rightarrow {}^7F_1$ [8, 14].

For spinels with gallium MAGS1 and MAGS2, the intensity of europium luminescence in the bands at 615, 690 nm is significantly higher in the samples obtained in the "scanning" mode. It is possible that europium ions are more effectively incorporated into the spinel lattice with gallium during synthesis in this mode.

Conclusions

The work shows that it is possible to synthesize luminescent porous ceramics based on spinels $MgAl_2O_4$, $MgAlGaO_4$ by means of the action of powerful flows of high-energy electrons with an energy of

1.4 MeV and a power of 7–30 kW / cm^2 directly on a batch of powders of metal oxides MgO, Al_2O_3, Ga_2O_3 in a stoichiometric ratio with activators europium oxide. The efficiency of radiation synthesis of spinel samples depends on the history of the initial oxide powder compositions. A mixture of oxide powders with close average particle sizes and similar particle distributions in the synthesis of ceramics by the radiation method gives a useful yield of up to 97 %. The particle size of about 5–10 μm, close average particle size and similar particle size distribution for various components of the batch is optimal for ensuring high efficiency of radiation synthesis

The structural and luminescent properties of spinel ceramic samples have been studied. The study revealed that Eu^{3+} ions are incorporated into the crystal lattice of both types of spinels. In the luminescence spectra of the synthesized spinel samples, luminescence of Eu^{3+} ions can be observed ($^5D_0$, $^5D_1 \rightarrow {}^7F_J$ transitions). The characteristic luminescent properties of the Eu^{3+} ion arise in the strongest spectral band at 615 nm ($^5D_0 \rightarrow {}^7F_2$ transition), which is more distinct in $MgAlGaO_4$ and $MgAl_2O_4$ samples synthesized from a mixture of oxide powders with a similar average particle size and granulometric composition. Superposition of the luminescence bands of chromium and europium ions ($^5D_0 \rightarrow {}^7F_4$ transition) is due to effective luminescence of chromium in the spectra of MAS1 and MAS2 samples excited by electrons. The emission peaks of the PL and CL spectra in MGAS1, MGAS2, MAS3 and MAS4 samples are similar; however, the PL spectrum of MAS1 and MAS2 samples does not exhibit a maximum peak at 690 nm compared to the CL spectrum.

Acknowledgments

The research was carried out at the expense of the grant of the Russian Science Foundation No. 23-73-00108, https://rscf.ru/project/23-73-00108/

The research was carried out using the equipment of the CSU NMNT TPU.

References

1 Goldstein A. Correlation between $MgAl_2O_4$-spinel structure, processing factors and functional properties of transparent parts (progress review) / A. Goldstein // J. European Ceramic Society. — 2012. — Vol. 32, No. 11. — P. 2869–2886. DOI: 10.1016/j.jeurceramsoc.2012.02.051

2 Pilania G. Prediction of structure and cation ordering in an ordered normal-inverse double spinel / G. Pilania, V. Kocevski, J.A. Valdez, C.R. Kreller, B.P. Uberuaga // Communication Materials. — 2024. — No. 84. DOI: https://doi.org/10.1038/s43246-020-00082-2

3 Tomokazu Ito Site Preference of Cations and Structural Variation in MgAl2–xGaxO4 (0≤x≤2) Spinel Solid Solution / Tomokazu Ito, Akihiko Nakatsuka, Hideki Maekawa, Akira Yoshiasa, Takamitsu Yamanaka // Zeitschrift für anorganische und allgemeine Chemie. — 2000. — Vol. 626, No. 1. — P. 42–49. DOI: https://doi.org/10.1002/(SICI)1521-3749(200001)626:1<42::AID-ZAAC42>3.0.CO;2-O

4 Kushwaha A.K. Structural, electronic, elastic and optical properties of double spinel $MgAlGaO_4$: a DFT investigation / Kushwaha, A.K., Güler, E., Özdemir, A. Genç A. E., Uğur G. // Indian J Phys. — 2024. — Vol. 98. — P. 4011–4017. DOI: https://doi.org/10.1007/s12648-024-03171-x

5 Luchechko A. Luminescence spectroscopy of Eu3+ and Mn2+ ions in MgGa2O4 spinel / A. Luchechko, O. Kravets, L. Kostyk, O. Tsvetkova // Radiation Measurements. — 2016. — Vol. 90. — P. 47–50. DOI: 10.1016/j.radmeas.2015.12.003

6 Bin-Siang T. Preparation and luminescent characteristics of Eu3+-activated MgxZn1−xGa2O4 nanocrystals / T. Bin-Siang, C. Yen-Hwei, C. Yu-Chung // Journal of Alloys and Compounds. — 2006. — Vol. 407. — P. 289–293. DOI: 10.1016/j.jallcom.2005.06.021

7 Jiang Bin. A self-activated MgGa2O4 for persistent luminescence phosphor / Bin Jiang, Fengfeng Chi, Xiantao Wei, Yonghu Chen, Min Yin // J. Appl. Phys. — 2018. — Vol. 124. — P. 063101. DOI: https://doi.org/10.1063/1.5024771

8 Yoon S.J. Synthesis and photoluminescence properties of $MgAl_2O_4$: Eu^{3+} phosphors / S.J. Yoon, D.A. Hakeem, K. Park // Ceramics International. — 2016. — Vol. 42. — P. 1261–1266. DOI: http://dx.doi.org/10.1016/j.ceramint.2015.09.059

9 Lisitsyn V. Radiation Synthesis of High-Temperature Wide-Bandgap Ceramics / V. Lisitsyn, A. Tulegenova, M. Golkovski, E. Polisadova, L. Lisitsyna, D. Mussakhanov, and G. Alpyssova // Micromachines. — 2023. — Vol. 14, No. 12. — P. 2193. DOI: 10.3390/mi14122193.

10 Lisitsyn V. Efficiency Dependence of Radiation-Assisted Ceramic Synthesis Based on Metal Oxides and Fluorides on Initial Powder Particle Sizes / V. Lisitsyn, E.Polisadova, L. Lisitsyna, A. Tulegenova, I. Denisov, M. Golkovski // Photonics. — 2023. – Vol. 10, No. 10. P.1084. DOI: https://doi.org/10.3390/photonics10101084

11 Kuksanov N. High Power DC Electron Accelerators of ELV-Type for Research and Industrial Application / N. Kuksanov, Yu. Golubenko, A. Lavruchin, D. Kogut, I. Chakin, S. Fadeev, P. Nemytov, A. Semenov, E. Domarov, V. Cherepkov, R. Salimov, A. Korchagin, M. Golkovsky, D. Vorobiev // 7th International Congress on Energy Fluxes and Radiation Effects (EFRE), Tomsk, Russia. — 2020. — P. 449–454. DOI: 10.1109/EFRE47760.2020.9241934.

12 Lisitsyn V. The Optimization of Radiation Synthesis Modes for YAG: Ce Ceramics / V. Lisitsyn, D. Mussakhanov, A. Tulegenova, E. Kaneva, L. Lisitsyna, M. Golkovski, A. Zhunusbekov // Materials. — 2023. — Vol. 16. — P. 3158 doi: https://doi.org/10.3390/ma16083158

13 Polisadova E.F. Pulse Cathodoluminescence of the Impurity Centers in Ceramics Based on the $MgAl_2O_4$ Spinel / E.F. Polisadova, V.A. Vaganov, S.A. Stepanov, V.D. Paygin, O.L. Khasanov, E.S. Dvilis, D.T. Valiev. R.G. Kalinin // Journal of Applied Spectroscopy. — 2018. Vol. 85. — P. 416–421. DOI: 10.1007/s10812-018-0666-9.

14 Gupta S.K. Why host to dopant energy transfer is absent in the $MgAl_2O_4$: Eu^{3+} spinel? And exploring Eu^{3+} site distribution and local symmetry through its photoluminescence: interplay of experiment and theory / S.K. Gupta, P.S. Ghosh, N. Pathaka, R.M. Kadam // RSC Advances. — 2016. — Vol. 6. — P. 42923–42932. DOI: https://doi.org/10.1039/C6RA03369E

15 Galazka, Z. $MgGa_2O_4$ as a new wide bandgap transparent semiconducting oxide: growth and properties of bulk single crystals / Z. Galazka, D. Klimm, K. Irmscher, R. Uecker, M. Pietsch, R. Bertram, M. Naumann, M. Albrecht, A. Kwasniewski, R. Schewski, M. Bickermann // Physica status solidi (a). — 2015. — Vol. 212. — P. 1455–1460. DOI: 10.1002/pssa.201431835.

16 Sawai S. Visible photoluminescence from $MgAl_2O_4$ spinel with cation disorder and oxygen vacancy / S. Sawai, T. Uchino // Journal of Applied Physics. — 2012. — Vol. 112. — P. 103523. DOI: https://doi.org/10.1063/1.4767228

17 Li Y. Monochromatic blue-green and red emission of rare-earth ions in $MgGa_2O_4$ spinel / Y. Li, P. Niu, L. Hu, X. Xu, C. Tang // Journal of Luminescence. — 2009. — Vol. 129. — P. 1204–1206. DOI: https://doi.org/10.1016/j.jlumin.2009.06.005

Е.Ф. Полисадова, Н.Д. Чан

Еуропиймен легирленген $MgAl_2O_4$ және $MgAlGaO_4$ кеуекті керамиканың құрылымы мен люминесценттік қасиеттерін электронды сәулені қолдана отырып синтездеу

Еуропиймен легирленген $MgAl_2O_4$ (MAS) және $MgAlGaO_4$ (MAGS) кеуекті керамикасы радиациялық әдіспен синтезделді. Радиациялық синтез синтезді ынталандыру үшін қоспаларды немесе басқа материалдарды пайдаланбай, оксид ұнтақтарының қоспасынан электронды іске қосу мен шихтаның сәулелену энергиясын пайдалана отырып, 1 секундтан аз уақыт ішінде жоғары тиімділікпен жүзеге асырылады. Жоғары энергиялы электронды сәулені қолдана отырып, синтездеу әдісі жоғары өнімділігі бар отқа төзімді материалдарды алуға, процестің технологиялық жағдайларын басқаруға және сәйкесінше берілген қасиеттері бар материалдарды синтездеуге мүмкіндік береді. Синтезделген кеуекті керамиканың құрылымдық қасиеттері рентгендік дифракция әдісімен (XRD-7000s дифрактометрі, Shimadzu), сканерлеуші электронды микроскопия әдістерімен зерттелген. Нәтижелер синтезделген MAS текше құрылымды және $MgAl_2O_4$ шпинелінің кристалдық құрылымына сәйкес келетінін көрсетті, ал MAGS синтезделген қос шпинельді екі негізгі фазалық компоненттен тұрады: $MgAl_2O_4$ және $MgGa_2O_4$. Еуропий қосылған синтезделген шпинельдің MAS және MAGS люминесценция қасиеттерін зерттеу үшін фотолюминесценцияны өлшеу жүргізілді. Шпинельдегі Eu^{3+} иондарының қозуының фотолюминесценция спектрі λ_{em} = 615 нм ($^5D_0 \rightarrow {}^7F_2$) кезінде бақыланды. PLE Eu^{3+} иондарының конфигурациясындағы f→f ауысуын көрсетеді 393 нм ($^7F_0 \rightarrow {}^5L_6$), 463 нм ($^7F_0 \rightarrow {}^5D_2$)). 330 нм және 260 нм-дегі қозу диапазоны Eu^{3+} және O^{2-} иондары арасындағы зарядтың ауысуына тән. 260 нм қозған үлгілердің фотолюминесценция спектрі зерттелді. Шпинель үлгілерінің PL спектрінде Eu^{3+} иондарының эмиссиясы айқын көрінеді. Ең көбі 615 диапазонының құрылымында шыңы 590 нм-де көрінеді, $^5D_0 \rightarrow {}^7F_1$ ауысуымен сипатталады. Үлгілердің ФЛ спектрінде $^5D_1$–$^7F_1$ ауысуымен Eu^{3+} иондарының шығарылуына тән максимум 535 нм болатын әлсіз спектрлік диапазон пайда болады. Радиациялық синтездің тиімділігі бастапқы оксид ұнтақтарының гранулометриялық құрамына байланысты екендігі көрсетілген.

Кілт сөздер: керамикалық шпинель, қос шпинель, Eu легирлеу, радиациялық синтез, люминесценция, $MgAl_2O_4$, $MgAlGaO_4$.

Е.Ф. Полисадова, Н.Д. Чан

Синтез с использованием электронного пучка, структура и люминесцентные свойства пористой керамики $MgAl_2O_4$ и $MgAlGaO_4$, легированной европием

Пористая керамика $MgAl_2O_4$ (MAS) и $MgAlGaO_4$ (MAGS), легированная европием, синтезирована радиационным методом. Радиационный синтез осуществлен с высокой эффективностью в течение менее 1 сек с применением энергии излучения электронного пуска и шихты из смеси порошков оксидов без использования добавок или других материалов для стимуляции синтеза. Метод синтеза с применением высокоэнергетического электронного пучка позволяет получать тугоплавкие материалы с высокой

производительностью, управлять технологическими условиями процесса и, соответственно, синтезировать материалы с заданными свойствами. Структурные свойства синтезированной пористой керамики исследованы методом рентгеновской дифракции (дифрактометр XRD–7000S, Shimadzu), методами сканирующей электронной микроскопии. Результаты показали, что синтезированные MAS имеют кубическую структуру и соответствуют в кристаллической структуре шпинели $MgAl_2O_4$, в то время как синтезированная двойная шинель MAGS содержит два основных фазовых компонента: $MgAl_2O_4$ и $MgGa_2O_4$. Для изучения люминесцентных свойств синтезированных MAS и MAGS шпинели, легированной европием, были проведены измерения фотолюминесценции (ФЛ). Спектр фотолюминесценции возбуждения ионов Eu^{3+} в шпинели контролировался при λ_{em} = 615 нм ($^5D_0 \rightarrow {}^7F_2$). ФЛ показывает переход f→f в конфигурации ионов Eu^{3+} (при 393 нм ($^7F_0 \rightarrow {}^5L_6$), 463 нм ($^7F_0 \rightarrow {}^5D_2$)). Полосы возбуждения при 330 нм и 260 нм характерны для зарядового перехода между ионами Eu^{3+} и O^{2-}. Изучен спектр фотолюминесценции образцов при возбуждении при 260 нм. В спектре ФЛ образцов шпинели отчетливо видно излучение ионов Eu^{3+}. В структуре полосы с максимумом 615 виден пик при 590 нм, характеризующийся переходом $^5D_0 \rightarrow {}^7F_1$. В спектре ФЛ образцов появляется слабая спектральная полоса с максимумом при 535 нм, характерная для излучения ионов Eu^{3+} с переходом $^5D_1$–$^7F_1$. Показано, что эффективность радиационного синтеза зависит от гранулометрического состава исходных порошков оксидов.

Ключевые слова: шпинель керамическая, двойная шпинель, легирование Eu, радиационный синтез, люминесценция, $MgAl_2O_4$, $MgAlGaO_4$.

References

1 Goldstein, A. (2012). Correlation between MgAl2O4-spinel structure, processing factors and functional properties of transparent parts (progress review). *J. European Ceramic Society, 32*(11), 2869–2886.

2 Pilania, G., Kocevski, V., Valdez, J.A., Kreller, C.R., & Uberuaga, B.P. (2024). Prediction of structure and cation ordering in an ordered normal-inverse double spinel. *Communication Materials, 84.*

3 Tomokazu, Ito, Akihiko, Nakatsuka, Hideki, Maekawa, Akira, Yoshiasa, & Takamitsu, Yamanaka (2000). Site Preference of Cations and Structural Variation in MgAl2–xGaxO4 (0≤x≤2) Spinel Solid Solution. *Zeitschrift fur anorganische und allgemeine Chemie, 626* (1), 42–49.

4 Kushwaha, A.K., Güler, E., Özdemir, A. Genç, A. E., & Uğur, G. (2024). Structural, electronic, elastic and optical properties of double spinel $MgAlGaO_4$: a DFT investigation. *Indian J Phys., 98*, 4011–4017.

5 Luchechko, A., Kravets, O., Kostyk, L., & Tsvetkova, O. (2016). Luminescence spectroscopy of Eu3+ and Mn2+ ions in MgGa2O4 spinel. *Radiation Measurements, 90,* 47–50.

6 Bin-Siang, T., Yen-Hwei, C., & Yu-Chung, C. (2006). Preparation and luminescent characteristics of Eu3+-activated MgxZn1−xGa2O4 nanocrystals. *Journal of Alloys and Compounds, 407,* 289–293.

7 Bin, Jiang, Fengfeng, Chi, Xiantao, Wei, Yonghu, Chen, & Min, Yin (2018). A self-activated MgGa2O4 for persistent luminescence phosphor. *J. Appl. Phys., 124,* 063101.

8 Yoon, S.J., Hakeem, D.A., & Park, K. (2016). Synthesis and photoluminescence properties of $MgAl_2O_4$: Eu^{3+} phosphors. *Ceramics International, 42,* 1261–1266.

9 Lisitsyn, V., Tulegenova, A., Golkovski, M., Polisadova, E., Lisitsyna, L., Mussakhanov, D., & Alpyssova, G. (2023). Radiation Synthesis of High-Temperature Wide-Bandgap Ceramics. *Micromachines, 14* (12), 2193.

10 Lisitsyn, V., Polisadova, E., Lisitsyna, L., Tulegenova, A., & Denisov, I., Golkovski, M. (2023). Efficiency Dependence of Radiation-Assisted Ceramic Synthesis Based on Metal Oxides and Fluorides on Initial Powder Particle Sizes. *Photonics, 10* (10), 1084.

11 Kuksanov, N., Golubenko, Yu., Lavruchin, A. et al. (2020). High Power DC Electron Accelerators of ELV-Type for Research and Industrial Application. *7th International Congress on Energy Fluxes and Radiation Effects (EFRE),* 449–454. Tomsk, Russia.

12 Lisitsyn, V., Mussakhanov, D., Tulegenova, A., Kaneva, E., Lisitsyna, L., Golkovski, M., & Zhunusbekov, A. (2023). The Optimization of Radiation Synthesis Modes for YAG: Ce Ceramics. *Materials, 16,* 3158.

13 Polisadova, E.F., Vaganov, V.A., Stepanov, S.A. et al. (2018). Pulse Cathodoluminescence of the Impurity Centers in Ceramics Based on the $MgAl_2O_4$ Spinel. *Journal of Applied Spectroscopy, 85,* 416–421.

14 Gupta, S.K., Ghosh, P.S., Pathaka, N., & Kadam, R.M. (2016). Why host to dopant energy transfer is absent in the $MgAl_2O_4$: Eu^{3+} spinel? And exploring Eu^{3+} site distribution and local symmetry through its photoluminescence: interplay of experiment and theory. *RSC Advances, 6,* 42923–42932.

15 Galazka, Z., Klimm, D., & Irmscher, K. et al. (2015). $MgGa_2O_4$ as a new wide bandgap transparent semiconducting oxide: growth and properties of bulk single crystals. *Physica status solidi (a), 212,* 1455–1460.

16 Sawai, S., & Uchino, T. (2012). Visible photoluminescence from $MgAl_2O_4$ spinel with cation disorder and oxygen vacancy. *Journal of Applied Physics, 112,* 103523.

17 Li, Y., Niu, P., Hu, L., Xu, X., & Tang, C. (2009). Monochromatic blue-green and red emission of rare-earth ions in $MgGa_2O_4$ spinel. *Journal of Luminescence, 129,* 1204–1206.

Information about the authors

Elena Polisadova (corresponding author) — Doctor of physical and mathematical sciences, Professor, National Research Tomsk Polytechnic University, Lenin av., 30, 634050, Tomsk, Russia; e-mail: *elp@tpu.ru*; https://orcid.org/0000-0002-4644-5967

Tran Nhan Dat — PhD student, National Research Tomsk Polytechnic University, Lenin av., 30, 634050, Tomsk, Russia; e-mail: *nhandattran94@gmail.com;* https://orcid.org/0000-0002-0710-5863